

# Overview on high frequency quasi-coherent modes at Wendelstein-7X

A.Krämer-Flecken<sup>1</sup>, J.H.E.Proll<sup>2</sup>, A.von Stechow<sup>2</sup>, G.Weir<sup>2</sup>, J-P.Böhner<sup>2</sup>, S.De Koker<sup>2,3</sup>,  
E.Edlund<sup>4</sup>, G.Fuchert<sup>2</sup>, J.Geiger<sup>2</sup>, O.Grulke<sup>2</sup>, X.Han<sup>5</sup>, M.Porkolab<sup>6</sup>, J.Smoniewski<sup>6</sup>,  
H.Trimiño Mora<sup>2</sup>, T.Windisch<sup>2</sup> and the W7-X Team

<sup>1</sup>*Institut for Fusion and Nuclear Waste Management, IFN-1, FZJ, Jülich, Germany* <sup>2</sup>*Max Planck Institut für Plasmaphysik, Greifswald, Germany* <sup>3</sup>*University of Greifswald, Greifswald, Germany* <sup>4</sup>*SUNY Cortland, Cortland, NY 13045, USA* <sup>5</sup>*University of Wisconsin - Madison, Madison, WI 53706 USA* <sup>6</sup>*Plasma Science and Fusion Center, MIT, Cambridge USA*

## Motivation

Wendelstein 7-X (W7-X) is the world's largest stellarator and optimized to minimize neo-classical transport. Turbulent transport governs heat- and particle-transport, driven mainly by the gradients in the electron-, ion- and density profiles. The ratio of the gradients, defined by  $\eta_e = L_n/L_{T_e}$  and  $\eta_i = L_n/L_{T_i}$ , where  $L$  denotes the gradient scale length, is found to be of particular importance in determining which type of turbulence dominates. Certain constraints on  $\eta_e$  and  $\eta_i$  determine which kind of turbulence dominates. The two most important types are the  $\nabla T_i$  driven turbulence (ITG) and the trapped electron mode (TEM) driven turbulence. The latter is excited within magnetic wells along a magnetic field line and becomes stabilized with increasing collisionality. TEM activity splits into electron-temperature-gradient-driven TEMs ( $\nabla T_e$ -TEMs) and density-gradient-driven TEMs ( $\nabla n_e$ -TEMs).

From the observation of turbulence diagnostic mode structure and phase velocity can be determined which give information on the wave number and the  $k_{\perp}\rho_s$  which allow separating ITG and TEM turbulence. The latter is observed for  $k_{\perp}\rho_s \geq 0.7$  and the ITG driven turbulence for  $k_{\perp}\rho_s \leq 0.5$ . Together with the profile analysis it is possible to determine the type of turbulence. This paper classifies high-frequency quasi-coherent modes (QCMs) observed at W7-X for different plasma parameters

## Diagnostic

Electron temperature and density profiles are measured by Thomson scattering [1]; ion temperature ( $T_i$ ) profiles by XICS [2]. For the identification of the mode structures the poloidal correlation reflectometer (PCR) [3] and the phase contrast imaging diagnostic (PCI) [4] are used, which also yield the poloidal rotation of the plasma and the determination of a possible phase velocity of the modes with respect to the  $E \times B$ -velocity. The PCR probes 6 different poloidal distances suppressing with the correlation condition between antenna pairs the uncorrelated background turbulence.

## Experimental observations in standard configuration

During power scan experiments (5 MW to 1 MW) at a medium line integrated density of  $n_e \approx 6 \times 10^{19} \text{ m}^{-3}$  and low collisionality, strong coherent structures appear in the PCR within  $0.4 \leq \rho \leq 0.7$  ( $\rho = r_{eff}/a$ ). A reflectometer scan across the gradient region reveals a broad coherent structure (fig.1) with a centre frequency of 230 kHz and a width of  $\Delta f = 130 \text{ kHz}$ . The centre

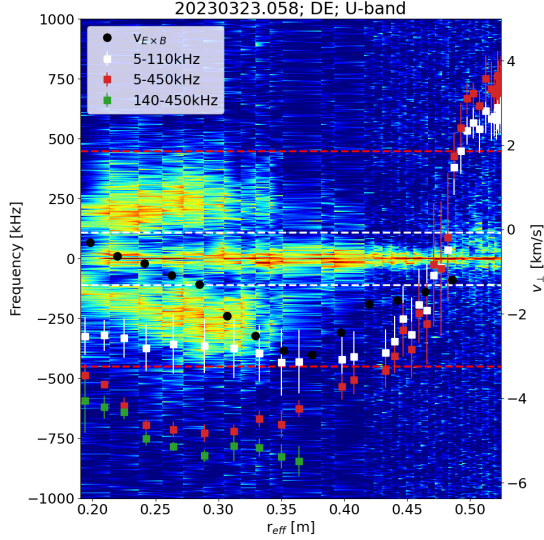


Figure 1: *Coherence spectrogram for  $s \approx 17 \text{ mm}$ , with quasi coherent modes for  $r_{eff} \leq 0.35 \text{ m}$ . Rotation for different filter intervals and the neoclassical  $E \times B$  -rotation are overlaid*

frequency increases with  $P_{ECRH}$  and  $\nabla T_e$ , respectively [5]. Due to the large half width of the structure they are called quasi coherent modes (QCMs). For the different frequency components (i) 5 kHz to 110 kHz corresponding to the low frequency turbulence (LF) and (ii) 140 kHz to 450 kHz the QCM range, a cross-correlation analysis yields the time delay of the propagation. Applying the elliptical model yields the poloidal velocity ( $v_{\perp}$ ) which is estimated to  $3.5 \text{ km s}^{-1}$  and  $5.5 \text{ km s}^{-1}$  for the different frequency intervals and for  $r_{eff} \leq 0.35 \text{ m}$ . The agreement between the LF turbulence and the neoclassical rotation outside the QCM region, confirms a sufficiently low phase velocity of the LF-turbulence to serve as a proxy for the  $E \times B$ -rotation. For the interval with QCMs, the increased  $v_{\perp}$  compared to  $E \times B$ -rotation indicates a propagation in electron diamagnetic drift direction, as expected for TEMs.

From the analysis of the coherence spectra for different distances the poloidal correlation length ( $L_{\perp}$ ) is estimated (see fig. 2) to  $L_{\perp} = 25(2) \text{ mm}$ . With  $\rho_s = 4 \text{ mm}$  to  $5 \text{ mm}$ ,  $L_{\perp}$  is in the range of  $3 - 10\rho_s$ , expected for  $\nabla T_e$ -TEMs. Knowing the circumference of the flux tubes covering the radii with QCMs, the calculated poloidal mode number is estimated to range from

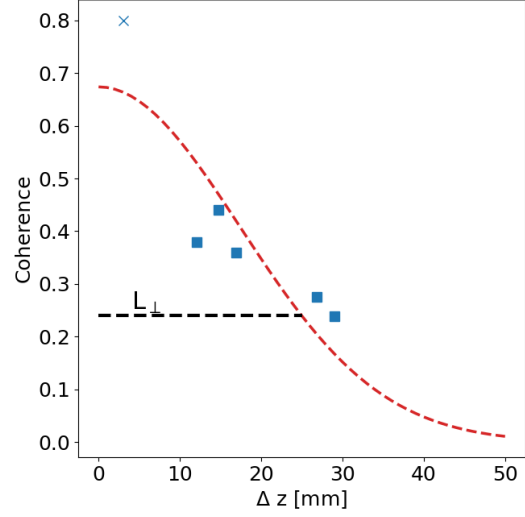


Figure 2: *Estimated  $L_{\perp}$  for QCM. Only those combinations can be considered, where both, QCM and LF-turbulence are visible. Contributions of broad band turbulence showing up at short time scales are neglected.*

$80 \leq m \leq 120$ , in agreement with  $\nabla T_e$ -TEMs. Also, the mean calculated  $k_{\perp} \rho_s$ -value of 1.35 fulfils the condition for  $\nabla T_e$ -TEMs. From the profile data a check of  $\eta_e$  and  $\eta_i$  for the radii with QCM-activity yields  $8 \leq \eta_e \leq 10$  reflecting the impact of  $\nabla T_e$  and confirms  $\nabla T_e$ -TEMs (fig.3). In contradiction  $\eta_i$  shows almost no variation and  $\bar{\eta}_i \approx 3.5$  is not sufficient for stabilizing ITG turbulence in low collisionality plasmas. Beside the QCM modes in the plasma core high fre-

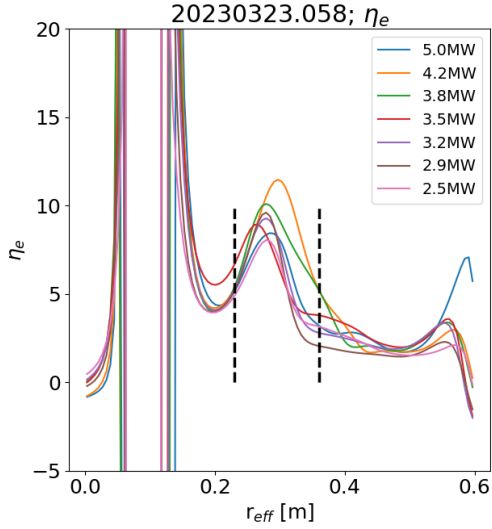


Figure 3:  $\eta_e$  for different power levels showing the influence of  $\nabla T_e$ . The dashed black lines mark the range with QCM activity.

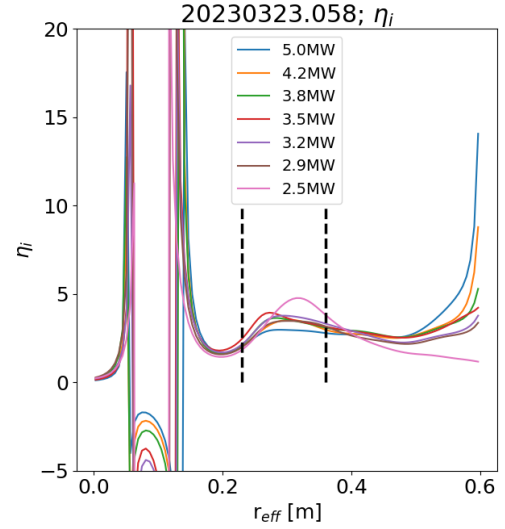


Figure 4:  $\eta_i$  for different power levels: no change in  $L_n/L_{T_i}$ .  $\eta_i$  is too large in the QCM region to stabilize ITG turbulence.

quency QCM modes are found in plasmas with steep density gradients [6]. These modes are observed in (i) NBI-fuelled or (ii) pellet fuelled plasmas. These QCMs are more located in the plasma edge at  $0.67 \leq r_{eff}/a \leq 0.77$  and observed in PCR as well as in phase contrast imaging (PCI). In fig. 5 the grey rectangle show the QCM activity within a full scan of the PCR ranging from the edge to the core and back. The frequency of the mode is higher compared to QCMs driven by  $\nabla T_e$  (see fig. 1) ranging from 700 kHz to 1100 kHz and increases with  $\nabla n_e$  and  $\nabla T_e$  (see fig. 6). At constant  $P_{ECRH}$  from 3 s to 8 s the density peaking is slowly increasing. With ramping up  $P_{ECRH}$  the peaking becomes significant as well as the increase of the QCM frequency. From the spectrogram the LF-turbulence and the QC-modes are well separated, and a cross-correlation analysis can be performed for the different frequency intervals. Compared to the LF-turbulence ( $v_{\perp} = -5 \text{ km s}^{-1}$ ) the QCM rotate at a higher velocity ( $v_{\perp} = -7.5 \text{ km s}^{-1}$ ) as expected for TEMs in general. An estimate of the  $L_{\perp}$  yields  $22 \text{ mm} \leq L_{\perp} \leq 27 \text{ mm}$ , similar to the  $L_{\perp}$  for QCMs from  $\nabla T_e$ -TEMs. With  $\bar{\rho}_s = 3.4 \text{ mm}$   $k_{\perp} \rho_s$  is in the range of 0.8 to 1.0 and within the range for  $\nabla n_e$ -TEMs. In addition, QCM activity goes along with an increase of the diamagnetic energy ( $W_{dia}$ ) of the plasma, and the so-called  $T_i$  clamping is surpassed [7]. Analysing  $\eta_e$ - and  $\eta_i$ -profiles for the region with mode activity yields  $\bar{\eta}_e = 1.4$ , slightly above  $\eta_e \lesssim 1.0$  ex-

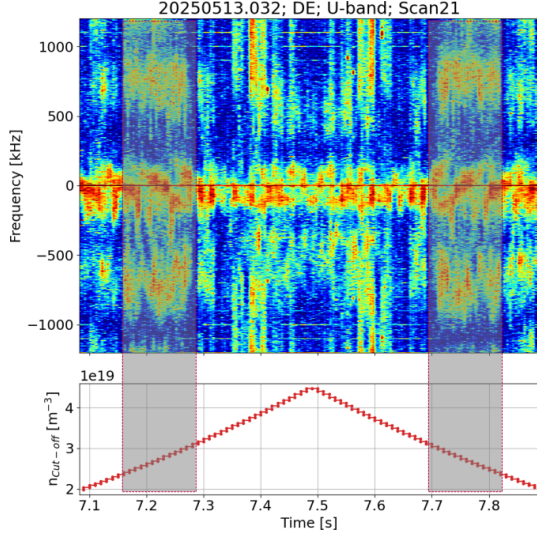


Figure 5: *Coherence spectrogram for  $s \approx 17$  mm, with QCMs in the greyish rectangles.*

pected for purely  $\nabla n_e$  driven TEMs in the plasma edge and suggest that both gradients  $\nabla T_e$  and  $\nabla n_e$  contribute. For these conditions ITG-turbulence is stabilized for  $\eta_i \leq 2/3$  and  $\bar{\eta}_i = 1.2$  is 3 times smaller than the value for the  $\nabla T_e$ -TEMs (see above), suggesting partly stabilized ITG-turbulence, in agreement with the increased  $W_{dia}$  and the observed reduced turbulence level [8]. Experiments with an 5/5-island inside the last closed flux surface, show similar QCMs with increased  $W_{dia}$ , suggesting a relation between the appearance of  $\nabla n_e$ -TEMs and the suppression of ITG-turbulence.

## Conclusions

Density fluctuations in W7-X are monitored with PCR and PCI. Two distinct classes of quasi-coherent modes driven by trapped particles are identified. In purely heated ECRH-plasmas,  $\nabla T_e$  TEMs are located at mid-radius and the  $\eta_e$  increase with  $\nabla T_e$ .  $T_i$ -profiles stay below the clamping limit and  $\eta_i$  suggest no reduction of ITG-turbulence. In contrast to  $\nabla T_e$ -TEMs, the  $\nabla n_e$ -TEMs are observed when the density profile shape is varied due to NBI-fuelling or pellets. Saturation of  $\eta_e$ -values at low levels and  $\eta_i = 1.2$  suggest partly stabilized ITG turbulence, being a possible reason for the increased  $W_{dia}$  and a reduction in the turbulence level.

## References

- [1] E.Pasch et al., Rev. Sci. Instrum. **87** (2016) 11E729
- [2] A.Langenberg, Rev. Sci. Instrum. **89** (2018) 10G101
- [3] A.Krämer-Flecken et al., Nucl. Fusion **57** (2017) 066023
- [4] E.M.Edlund et al., Rev. Sci. Instrum. **89** (2018) 10E105
- [5] A.Krämer-Flecken et al., Plasma Phys. Control. Fusion **67** (2025) 025014
- [6] A.Krämer-Flecken et al., 25th Int. Stellarator–Heliotron Workshop, Cordoba (2026)
- [7] M.N.A.Beurskens et al., Nucl. Fusion **61** (2021) 116072
- [8] S.A.Bozhenkov et al., 2026 Plasma Phys. Control. Fusion **68** (2026) 055015

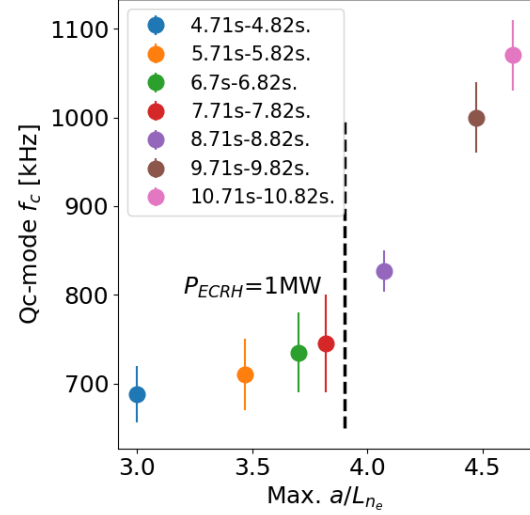


Figure 6: *Scaling of  $f_{QCM}$  with  $a/L_{n_e}$  showing a strong increase with  $P_{ECRH}$ .*